SPREADING OF THE OLYMPUS MONS VOLCANIC EDIFICE, MARS. P. J. McGovern[1] and J. K. Morgan[2], [1]Lunar and Planetary Institute, 3600 Bay Area Blvd., Houston TX 77058, USA (mcgovern@lpi.usra.edu), [2]Department of Earth Science, Rice University, Houston, TX 77005, USA (morganj@rice.edu).

Introduction: Olympus Mons on Mars is the tallest known volcano in the solar system, with height about 23 km above base and a diameter about 600 km. Recent topography and image data are consistent with suggestions [e.g., 1-4] that Olympus Mons has undergone the process of volcanic spreading, in which the flanks of the volcano move outward to accommodate intrusive and extrusive growth. However, this process appears to have different manifestations in different sectors of the edifice. Here, topographic profiles of Olympus Mons are compared to profiles generated by Distinct Element Method (DEM) models of volcanic spreading [4, 5]. Our goal is to evaluate the relative contributions of spreading to the volcano's structure and to infer the boundary conditions (i.e., high- or low-friction) at the base of the edifice.

Data: We take radial topographic profiles of Olympus Mons from the MOLA 1/128th degree gridded dataset [6], over 15 degree azimuth increments. We depart from previous practice in that the origin for the profiles is not the center of the summit caldera complex [e.g., 7], but rather at the area-averaged centroid of the quasi-circular 6 km topographic contour, located at 18.9N 226.0E, northwest of the caldera complex (Fig. 1). The 6 km contour can be regarded as the "edge" of the edifice because it tends to separate the gentle central slopes from the steeper ones of the Olympus Mons basal escarpment. Referencing the profiles to this "Center of Figure" (or COF) gives us a new perspective on the varying morphologies of the Olympus Mons edifice, in particular the contrast between the northwest and southeast quadrants.

With this new COF perspective, we see a stark contrast between the mean topographic profiles of the opposing southeast and northwest quadrants: the former (Fig. 2a, red line) contains the summit of the volcano, with topography well in excess of the overall mean profile, whereas the latter (Fig. 2a, blue line) falls well short of the all-azimuth average. The northwest mean profile shows continually decreasing slope with increasing radius, resulting in a concave-upward profile. In contrast, the southeast mean profile exhibits a nearly constant slope between the summit region and the base. The other pair of opposing quadrants, southwest and northeast, show mean profiles that are close to each other and to the overall mean profile (Fig. 2a).

Individual profiles from each quadrant yield more detail. The caldera complex and summit are visible in the azimuth 150 profile (Fig. 2b, red line), as are small topographic humps further outward in radius. The humps correspond to terraces, visible as the light or dark blue arcuate structures encircling the summit region in Fig. 1. The azimuth 330 profile (Fig. 2b, blue line) also cuts through terraces northwest of the caldera. The distribution of terraces is asymmetric with respect to both the caldera complex and the COF; they cover a much larger fraction of the southeastern flank than of the northwestern flank (Fig. 1).

Models: We used the Distinct Element Method (DEM) to model the growth of large volcanic edifices on Earth and Mars [4, 5]. The volcanoes are approximated as granular piles subject to frictional Coulomb failure criteria, allowing us to examine the effects of different internal and basal strength conditions. The edifices are constructed by "raining" particles from above, allowing them to settle onto a growing pile. The increased gravitational load following each increment of particles relaxes by particle avalanching down the surfaces (analogous to lava flows), and by internal faulting and deformation of the edifice, re-establishing the stress equilibrium of the edifice. Basal and internal friction parameters can vary spatially, leading to a rich variety of edifice morphologies and deformation behaviors that can be compared to Olympus Mons [4]. For example, piles built upon low basal friction substrates experience outward slip of their flanks, producing concave-upward topographic profiles that resemble the northwest Olympus Mons flank profile in Fig. 2. Models with high basal friction exhibit nearly constant angle slopes, resembling the lower southeast flank profile (i.e., beyond the summit region) in Fig. 2.

Discussion: The asymmetric structure of the Olympus Mons edifice with respect to its caldera has been noted for decades. The asymmetry has been attributed to slope effects of the neighboring Tharsis rise [e.g., 2], or as a remnant of even greater ancient asymmetry of proto-Olympus Mons, [e.g., 8]. The latter idea was proposed to explain the great lateral extent of the rough aureole deposits to the north and west of the edifice [8], but recent analysis suggests that such an elongated proto-edifice is neither volcanologically likely nor required to account for the aureoles [3].

In contrast, regional-scale topography is likely to affect spreading of volcano flanks. At Olympus Mons, Tharsis Rise slopes may "buttress" the southeastern flank of Olympus Mons [e.g., 2] thereby inhibiting flank movement in the same manner that Mauna Loa buttresses the younger and smaller Kilauea volcano

[9]. Regional topography may also play a role in setting the basal boundary condition for the edifice, a key factor in volcano growth [e.g., 2]. The scenario for flank spreading and failure at Olympus Mons given by [3] invokes pore fluid (water) trapped in an overpressurized basal layer, reducing the effective friction at the base of the volcano. The water may have been trapped in sediment layers deposited in the lowlands terrain that the Olympus Mons volcano formed on. However, terrain closer to the proto-Tharsis Rise may lack water-saturated sediments due to its higher elevation. Thus, flank segments closer to the ancient topographic rise may experience higher friction at their bases, yielding higher slopes (Fig. 2) and horizontal compressive stresses [2, 4, 5].

The circum-summit terraces seen in Fig. 1 have been attributed to thrust faults induced by compressional edifice stresses [10]. If the terraces are indeed thrust faults, their preponderance on the southeastern flank is consistent with inhibition of outward flank movement by the buttressing and pore fluid absence effects predicted to be in operation there (see above). The relative paucity of terraces on the northwest flank, as well as the characteristic concave-upward topographic profiles there (Fig. 2) are consistent with an absence of buttressing effects and the presence of a low-friction basal boundary condition.

We note that the outer boundary of the terraced region (Fig. 1) is roughly circular: the center of this circle is located to the southwest of the caldera, opposite from the COF but intriguingly very close to the topographic summit of the edifice. The offsets of the "terrace zone" centroid and topographic summit from the caldera complex may also result from the buttressing and pore-fluid-draining effects of the Tharsis rise, effects which favor steeper topography on the southwest flank. Alternatively (or additionally), perhaps a greater degree of horizontal compression in the southwest sector of the edifice causes lateral intrusions (sills) to be preferentially emplaced in that direction, thereby accounting for greater upward displacement of the summit to the southwest of the caldera.

References: [1] A. Borgia et al., *JGR, 95*, 14,357, 1990. [2] P. J. McGovern and S. C. Solomon, *JGR, 98*, 23,553, 1993. [3] P. J. McGovern et al., *JGR, 107*, doi10.1029/2004JE002258, 2004. [4] J. K. Morgan and P. J. McGovern, JGR, doi10.1029/2004JB003252, in press, 2005. [5] J. K. Morgan and P. J. McGovern, JGR, doi10.1029/2004JB003253, in press, 2005. [6] D. E. Smith et al., *JGR, 106*, 23,689, 2001. [7] P. J. McGovern et al., *LPS XXXIV*, abstract 2080, 2003. [8] P. W. Francis and G. Wadge *JGR, 88*, 9333, 1983. [9] Fiske and Jackson, Proc. Roy. Soc. Lond., Ser. A.,, 329, 299, 1972. [10] P. J. Thomas et al, JGR, 95, 14,345, 1990.

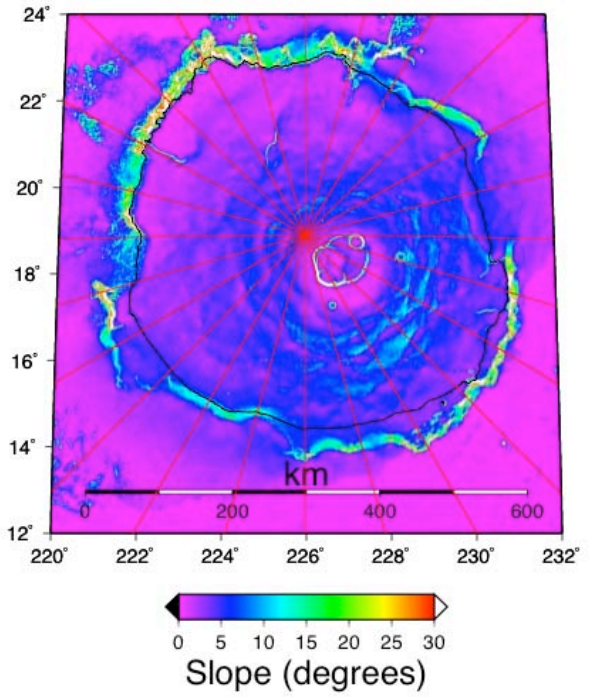

Figure 1. Slope map for the Olympus Mons edifice, (derived from the MOLA 1/128th degree gridded dataset [6]), showing the maximum value of slope at each point (in degrees). Ground tracks of topography profiles, at 15-degree azimuth intervals, are shown as red lines emanating from the "Center of Figure" (COF), the centroid of the region bounded by the 6 km topographic contour (black line).

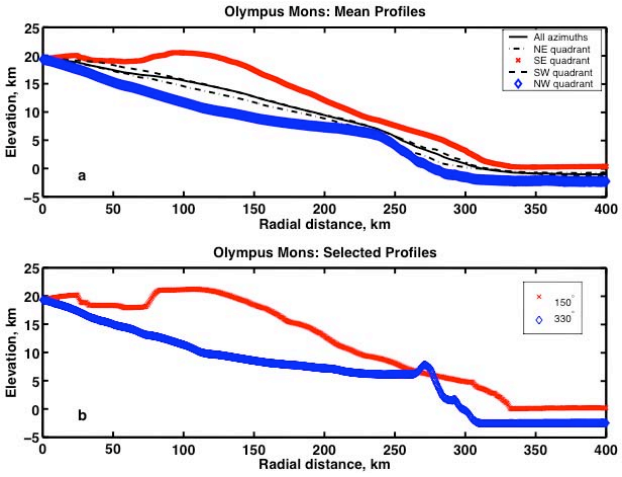

Figure 2. (a) Mean topographic profiles for four quadrants of the Olympus Mons volcanic edifice, with an overall mean profile (thin solid black line), based on the profile tracks shown in Figure 1. Southeast quadrant in red, northwest quadrant in blue. Northeast and southwest quadrants in black dot-dashed and dashed lines, respectively. (b) Topographic profiles for azimuths 150 (red) and 330 (blue).